

Sodium channel TRPM4 and sodium/calcium exchangers (NCX) cooperate in the control of Ca²⁺-induced mucin secretion from goblet cells

Gerard Cantero-Recasens^{1,2}, Cristian M. Butnaru^{1,2}, Nathalie Brouwers^{1,2}, Sandra Mitrovic³, Miguel A. Valverde⁴, Vivek Malhotra^{1,2,5,*}

From the ¹Centre for Genomic Regulation (CRG), The Barcelona Institute for Science and Technology, Dr. Aiguader 88, 08003 Barcelona, Spain; ²Universitat Pompeu Fabra (UPF), Barcelona, Spain; ³University Hospital of Basel, Clinical Chemistry, Petersgraben 4, 4031 Basel, Switzerland; ⁴Laboratory of Molecular Physiology, Faculty of Health and Life Sciences, Universitat Pompeu Fabra, 08003 Barcelona, Catalonia, Spain; ⁵Institució Catalana de Recerca i Estudis Avançats (ICREA), Pg. Lluís Companys 23, 08010 Barcelona, Spain

Running title: *TRPM4 and NCXs mediated mucin secretion*

*To whom correspondence should be addressed: Vivek Malhotra: Department of Cell and Developmental Biology, Centre for Genomic Regulation (CRG), Carrer Dr. Aiguader 88, 08003 Barcelona, Spain; vivek.malhotra@crg.eu; Tel. (+34) 93 316 02 35.

Keywords: MUC5AC, MUC2, NCX, TRPM4, TRPM5, goblet cell, cystic fibrosis

ABSTRACT

Regulated mucin secretion is essential for the formation of the mucus layer that protects the underlying epithelial cells from foreign particles. Alterations in the quantity or quality of secreted mucins are therefore detrimental to airway and colon physiology. Based on various biochemical assays in several human cell lines, we report here that Na⁺/Ca²⁺ exchanger 2 (NCX2) works in conjunction with transient receptor potential cation channel subfamily M member 4 (TRPM4), and perhaps TRPM5, Na⁺ channels to control Ca²⁺-mediated secretion of both mucin 2 (MUC2) and MUC5AC from HT29-18N2 colonic cancer cells. Differentiated normal bronchial epithelial (NHBE) cells and tracheal cells from patients with cystic fibrosis (CFT1-LC3) expressed only TRPM4 and all three isoforms of NCXs. Blocking the activity of TRPM4 or NCX proteins abrogated MUC5AC secretion from NHBE and CFT1-LC3 cells. Altogether, our findings reveal that NCX and TRPM4/TRPM5 are both required for mucin secretion. We therefore propose that these two proteins could be potential pharmacological targets to control mucus-related pathologies such as cystic fibrosis.

Human genome encodes 21 different mucin proteins that are secreted to compose the mucous layer, which protects the underlying tissue from pathogens, allergens and chemical agents (1). Of these mucins, Mucin 2 (MUC2), Mucin 5AC (MUC5AC) and Mucin 5B (MUC5B) are the best characterized gel-forming mucins (2). MUC2 is the major constituent of colonic mucus (3), whereas MUC5AC and MUC5B are the main mucins expressed in the airways (4).

Mucins of about 500 kDa are synthesized in the endoplasmic reticulum (ER) and transported to the Golgi complex where, after extensive glycosylation, these proteins can reach sizes of up to 2.5 million daltons (5, 6). After sorting at the Golgi, the heavily glycosylated mucins are packed into μm sized granules that mature to contain highly condensed mucins (2). The mechanism of mucin sorting and export at the Golgi are not known. Mucin containing granules undergo a process of maturation, which is accompanied by condensation of mucins. A pool of mature granules fuses to plasma membrane by two different pathways: 1, baseline or exogenous agonist independent reaction and 2, exogenous agonist dependent or the stimulated pathway.

The key issue in the late stages of mucin release pathways is to tightly regulate the number of granules that fuse to plasma membrane by SNARE dependent reaction. We have recently shown that baseline mucin secretion in colonic cancer cells, and in mouse colon *in vivo*, depends on KChIP3, a calcium sensor, and intracellular calcium oscillations. KChIP3, however, does not appear to have a role in the extracellular agonist dependent stimulated mucin secretion (7).

High levels of an extracellular stimulus (for example, ATP released in paracrine fashion and its metabolite adenosine, and possibly by inflammatory mediators) is well known to trigger mucin secretion by the involvement of a G protein-coupled receptor (like P2Y2) that activates phospholipase C to generate DAG, which activates PKC, and IP₃ that releases Ca²⁺ from apical ER (5). Activated PKC phosphorylates a protein called myristoylated alanine-rich C kinase substrate (MARCKS) on the cytoplasmic face of the plasma membrane (PM). This phosphorylation, or binding to Ca²⁺-Calmodulin, dissociates MARCKS from the PM, which is then recruited to mucin granules by Hsp70 and cysteine string protein (8). MARCKS bound granules then dock to the apical surface by an actin dependent process and fuse to plasma membrane by SNARE dependent fusion process, which involves VAMP8, SNAP23 and Munc18b (5, 9, 10). The syntaxin family member involved in this fusion reaction is not known.

TRPM5, a Ca²⁺-activated monovalent cation-selective channel, which is expressed in HT29-18N2 colonic cancer cell line, is required for stimulated MUC5AC secretion (11). While differentiated HT29-18N2 colonic cancer cells secrete MUC5AC, normal colonic cells secrete MUC2. Is TRPM5 required for MUC2 secretion by colon cells? Cells of the airways, on the other hand, secrete MUC5AC, but instead of TRPM5 express its close homolog TRPM4 (12, 13). Is TRPM4 required for MUC5AC release in the airways? We have shown previously that TRPM5 activation by ATP promotes calcium entry most likely via a Na⁺/Ca²⁺ exchanger (NCX) to trigger MUC5AC secretion from HT29-18N2 cells

(11). NCX is an antiporter membrane protein that uses energy from Na⁺ gradient across the plasma membrane to pump Ca²⁺ out of the cell against its large electrochemical gradient. However, depending on the electrochemical potential that determines the Na⁺ flux, NCX can work in two ways: in the forward mode, it promotes Ca²⁺ extrusion from the cell; while in the reverse mode, it allows Ca²⁺ entry into cells. Mammals express three genes encoding for NCX (*SLC8A1*, *SLC8A2* and *SLC8A3*) in a tissue-specific manner (reviewed in (14)). Which of these NCX isoforms specifically controls MUC2 and MUC5AC secretion? To address these issues we have investigated the role of TRPM4, TRPM5, and NCXs in stimulated mucin secretion from both colonic and airway cells.

Results

Expression of TRPM4, TRPM5 and NCX2 in HT29-18N2 colonic goblet cells

We used HT29-18N2 cells that differentiate into mucin producing cells after 6 days of incubation in protein-free medium as a means to unravel the requirements for MUC2 and MUC5AC secretion (11). These HT29-18N2 cells are a good model system to study MUC5AC and MUC2 secretion. We acknowledge the caveats that MUC5AC is not ordinarily expressed in gastrointestinal cells. It is also important to note that the expression levels of MUC2 might be different in HT29-18N2 compared to the physiologically relevant cells in the colon. Total mRNA was extracted from differentiated HT29-18N2 cells and expression of NCXs, TRPM4 and TRPM5 was monitored by reverse transcription of the mRNA and PCR with specific primers for each gene (Table 1). MUC5AC and MUC2 were used as positive controls for differentiation of HT29-18N2 cells, and respective control cDNA (MTC cDNA Panels, Clontech Laboratories) was used to test each set of primers (control cDNA for: NCX1, NCX2, TRPM4; lungs cDNA for: NCX3, TRPM5 and MUC5AC; colon cDNA for: MUC2). Our results show that TRPM4, TRPM5 (as shown before in (11)) and NCX2 (*SLC8A2* gene) are expressed in differentiated

HT29-18N2, whereas NCX1 and NCX3 (*SLC8A1* and *SLC8A3* genes, respectively) are not expressed in these cells (Figure 1A).

We generated shRNA-dependent HT29-18N2 cell lines stably depleted of TRPM4, TRPM4+TRPM5, or NCX2 as described in materials and methods. The HT29-18N2 cell line stably depleted of TRPM5 has been described previously (11). Knockdown efficiency estimated by qPCR revealed greater than 65% reduction of TRPM4 mRNA levels in TRPM4 KD cells (Figure S1A); 85% and 75% reduction in TRPM4 and TRPM5 mRNA levels, respectively, in TRPM4+TRPM5 KD cells (Figure S1B), and 60% reduction of NCX2 mRNA levels in NCX2 KD cells (Figure S1C). We also tested the effect of TRPM4 and TRPM5 shRNA on the expression of other transgenes. Our results show that TRPM4 shRNA did not affect TRPM5 levels (Figure S1A), however, TRPM5 shRNA produced a 60% decrease in TRPM4 levels (and 80% reduction of TRPM5 levels, as published in (11) (Figure S1D)).

MUC2 and MUC5AC secretion by HT29-18N2 goblet cells requires TRPM4/TRPM5 and NCX2

We first measured MUC5AC secretion in TRPM4 KD, TRPM5 KD (described previously (11)), TRPM4+TRPM5 KD and NCX2 KD cells, which were differentiated by serum starvation, and treated with 100 μ M ATP for 30 min at 37°C. Cells expressing TRPM4 or TRPM5 shRNA displayed a similar reduction of ATP-dependent MUC5AC secretion compared to control cells (36% and 33%, respectively). Interestingly, TRPM4+TRPM5 KD and NCX2 KD cells also presented comparable reduction in MUC5AC secretion compared to control cells (43% and 48% reduction) (Figure 1D). Next, we studied their role in ATP-mediated MUC2 secretion. Control and KD cells were differentiated and treated with 100 μ M ATP for 30 min at 37°C. As shown in Figure 1E, knockdown of TRPM4, TRPM5, TRPM4+TRPM5, and NCX2 strongly blocked MUC2 secretion (Figure 1E). Could the knockdown effects of these proteins on MUC2

and MUC5AC secretion be due to alteration in the total intracellular levels of the respective mucins? We addressed this potential issue by measuring intracellular mucin levels. The dot blot with anti-MUC5AC or anti-MUC2 antibody of total cell lysate from TRPM4 KD, TRPM5 KD, TRPM4+TRPM5 KD, NCX2 KD, and control cells revealed no obvious differences in the intracellular MUC5AC or MUC2 levels in any of the knockdown cells compared to control cells (Figure 1B and 1C). In addition, we examined the quantity and organization of intracellular MUC2 and MUC5AC granules by immunofluorescence microscopy (IF) with anti-MUC2 and anti-MUC5AC antibody, respectively. Our data show no obvious morphological differences, by fluorescence microscopy, in the distribution of MUC5AC or MUC2 secretory granules in TRPM4, TRPM5, TRPM4+TRPM5, and NCX2 depleted cells compared to control cells (Figure 1F).

NCX2 and TRPM4 control ATP-mediated Ca^{2+} entry into HT29-18N2 goblet cells

Mucin secretion is a Ca^{2+} dependent process. However, whether the source of Ca^{2+} is intracellular, extracellular or both is unclear (11, 15, 16). In the airways, PMA (phorbol-12-myristate-13-acetate) can trigger mucin secretion without any dependence on extracellular Ca^{2+} (15–17). We have reported previously that TRPM5 regulates extracellular Ca^{2+} entry, independent of VGCC (voltage gated calcium channels), and this event is essential for the physiological ATP-mediated mucin secretion from HT29-18N2 cells (11). Moreover, there is growing evidence on the requirement of extracellular Ca^{2+} for mucin secretion in different cell types under physiological conditions (18–20). It is likely that PMA, a DAG mimic, which strongly activates PKC (8), Munc-13 (21) and many other proteins (22, 23), can override the dependence on extracellular Ca^{2+} in contrast to physiological stimuli such as ATP, menthol, and cold. We therefore retested the role of external Ca^{2+} in ATP-dependent mucin secretion to understand the involvement of TRPM4/TRPM5 and NCX2.

First, we monitored ATP-dependent MUC5AC and MUC2 secretion in the presence (1.2 mM CaCl₂) or absence (0.5 mM EGTA) of extracellular Ca²⁺ (30 min at 37°C). Extracellular medium was collected and analyzed by dot blot with anti-MUC5AC and anti-MUC2 antibody, respectively. Quantification of the dot blot showed that both MUC5AC (Figure 2A) and MUC2 secretion (Figure 2B) requires extracellular Ca²⁺. This confirms our previous findings that MUC5AC secretion by ATP mediated pathway depends on extracellular Ca²⁺. ATP-mediated calcium entry is a combination of ROCE (Receptor Operated Calcium Entry, likely involving TRP channels) and SOCE (Store Operated Calcium Entry, dependent on Orai channels) (24). We used Thapsigargin (TG) to inhibit Sarco/endoplasmic reticulum Ca²⁺ ATPase (SERCA) (25), which ordinarily promotes Ca²⁺ release from ER and triggers SOCE. Our results show that TG triggered similar levels of calcium release from the ER and higher levels of calcium entry as observed after addition of 1.2 mM CaCl₂ to the extracellular medium compared to ATP stimulation (Figure 2C, quantification in 2D), but it did not promote MUC5AC secretion (Figure 2E). These data reveal that ATP-mediated Ca²⁺ release from intracellular stores (in the absence of extracellular Ca²⁺) or SOCE are insufficient to promote stimulated mucin secretion from HT29-18N2 cells. Extracellular Ca²⁺ entry (involving TRPM5 as shown previously (11)), is, however, necessary for both MUC5AC and MUC2 release.

Second, we measured intracellular Ca²⁺ levels with the calcium dye FURA-2AM in differentiated HT29-18N2 cells upon stimulation with 100 μM ATP. Our data confirm that in absence of extracellular Ca²⁺ (medium containing 0.5 mM EGTA), ATP triggered Ca²⁺ release from the intracellular stores, and, importantly, it promoted Ca²⁺ entry into the cells after addition of 1.2 mM CaCl₂ to the extracellular medium (Figure 2C, black symbols). We then tested whether TRPM4, TRPM5 and NCX2 had a role in ATP mediated Ca²⁺ entry into the cells. We measured intracellular Ca²⁺ levels in differentiated NCX2 KD, TRPM4 KD,

TRPM5 KD, TRPM4+TRPM5 KD, and control HT29-18N2 cells with the calcium dye FURA-2AM and 100 μM ATP as the stimulus (in the absence or presence of extracellular Ca²⁺).

Our data show that Ca²⁺ release from internal stores was not affected in any of the knockdown cells compared to control cells (Figure 2F), however, there was a clear reduction in Ca²⁺ entry after addition of extracellular Ca²⁺. Quantification of the data shown in figure 2F (Figure 2G) reveal a 20% reduction in Ca²⁺ entry for TRPM4 and TRPM5 KD cells, a 37.5% reduction for the TRPM4+TRPM5 KD cells, and a 40% reduction in NCX2 KD cells compared to control cells. Considering that both TRPM4 and TRPM5 are Na⁺ channels activated by similar stimuli (i.e. intracellular Ca²⁺ and PKC) (13), and NCX2 can promote Ca²⁺ entry by operating in the reverse mode (26), we suggest that functional coupling of TRPM4/TRPM5 and NCX2 facilitates reverse mode NCX activity. We do not claim a direct interaction of TRPM4/TRPM5 and NCX2, but we propose that TRPM4/TRPM5 and NCX2 are in the same pathway of ATP mediated calcium entry to promote mucin secretion from HT29-18N2 cells.

MUC5AC is secreted by differentiated airway cells

We tested whether TRPM4/TRPM5 and NCX have a role in mucin secretion in two different airway cell lines: 1) NHBE, normal human bronchial epithelial cells, and 2) CFT1-LC3 cells, a human tracheal epithelial cell line derived from a patient with cystic fibrosis (CF) presenting homozygous mutation ΔF508 in CFTR channel and transformed with human papilloma virus E6/E7 genes and a retroviral vector alone (27). CFT1-LC3 cells are used extensively to study defective hydroelectrolyte transport characteristic of CF (28). Patients with CF exhibit accumulation of sticky mucus in the lungs, pancreas, intestine, and reproductive organs. Because secreted mucins are a major component that control the rheological properties of mucus (2), understanding the pathway of mucin secretion could potentially provide new targets to

potentially alleviate symptoms associated with CF (29).

To study MUC5AC secretion by airway cells, we used the air liquid interface (ALI) procedure, which effectively promotes normal human tracheal and bronchial epithelial cells differentiation into mucin secreting cells (30). Briefly, airway epithelial cells are plated on a porous membrane to form a monolayer. The basal plasma membrane of these cells is exposed to the medium, whereas the apical surface faces the air. We used this standard protocol that includes incubation with interleukin-13 (IL-13) to differentiate NHBE and CFT1-LC3 cells into secretory goblet cells (See Figure 3A). To assess if both cell lines are differentiated into mucin producing cells by this protocol, we first tested the mRNA and protein levels of MUC5AC. Total RNA was extracted from undifferentiated differentiated NHBE and CFT1-LC3 cells, and expression of *MUC5AC* was tested by RT-PCR and qPCR using specific primers for *MUC5AC* (and *GAPDH* as reference gene). As shown in Figure 3B, *MUC5AC* levels in differentiated compared to undifferentiated NHBE and CFT1-LC3 cells increased by 3.5-fold and 3-fold, respectively (Figure 3B). MUC5AC protein levels were determined in cell lysates of undifferentiated and differentiated NHBE and CF cells, respectively, with specific anti-MUC5AC antibody by the dot blot procedure. Our data reveal that both NHBE and CFT1-LC3 cells upregulate MUC5AC protein levels upon differentiation compared to undifferentiated cells (Figure 3C). Finally, we used a combination of three different mucin secretagogues (100 μ M ATP, 10 ng/ml IL-13 and 300 nM PMA) (8, 11, 31) to trigger MUC5AC secretion. Although ATP is a potent stimulus for mucin secretion (16), we supplemented it with IL-13 (which stimulates MUC5AC expression and also increases its secretion) (31) and limiting quantities of PMA (strong activator of PKC and known to cause MUC5AC secretion) (8, 11) to increase the amount of MUC5AC secreted by both NHBE and CFT1-LC3 differentiated cells, thereby making it detection easier in the extracellular space. Importantly, only differentiated cells

secrete MUC5AC after stimulation with ATP, IL-13 and PMA (Figure 3D).

TRPM4 and NCX1/2/3 are expressed in differentiated airway cells

After differentiation, RNA from NHBE and CFT1-LC3 cells was extracted, retro-transcribed into cDNA and analyzed by PCR (primers in Table 1). Our results show that TRPM4, but not TRPM5, and all 3 members of NCX family (NCX1, NCX2 and NCX3) are expressed in differentiated NHBE and CFT1-LC3 cells. *MUC5AC* was detected as a positive control for differentiation of cells and *HPRT1* was used as a loading control (Figure 3E). Taken together, our findings reveal that both differentiated NHBE and CF-derived cells express specific members of TRPM4/TRPM5 and NCX family of proteins. We therefore tested whether NCX's reverse mode pathway is required for mucin secretion by these airway cells.

Inhibition of NCX's reverse mode blocks MUC5AC secretion in both NHBE and CF cells

To test the involvement of NCX in MUC5AC secretion, we applied the mix containing 100 μ M ATP, 10 ng/mL IL-13 and 300 nM PMA or a vehicle to CFT1-LC3 and NHBE cells (1 hr at 37°C). These exogenous stimuli promoted MUC5AC secretion from both NHBE and CFT1-LC3 differentiated cells (Figure 4A and 4B, control bars, respectively) compared to cells treated with the vehicle alone. We then tested whether inhibition of NCX's reverse mode affected mucin secretion from these cells by using a benzyloxyphenyl analog KB-R7943, which preferentially inhibits the NCX's reverse mode (34, 35, 36). Although KB-R7943 affects all 3 isoforms of human NCXs, it is 3-fold more effective in inhibiting NCX3 compared to its effects on NCX1 and NCX2 (33). Our results demonstrate that 50 μ M KB-R7943, a concentration previously described to inhibit NCX in HT29-18N2 cells (11), completely abolished MUC5AC secretion in NHBE and CFT1-LC3 differentiated cells (Figure 4A and 4B, respectively). We cannot rule out the possibility that KB-R7943 affects mucin

secretion by its effects on other membrane channels and transporters, but it is certainly not via SOCE (34), the N-methyl-D-aspartate receptor (35), neuronal nicotinic acetylcholine receptors (36), and the norepinephrine transporter (37) as none of these components are directly involved in MUC5AC secretion.

To further assess the involvement of NCX's reverse mode in MUC5AC secretion by CF cells, we tested the effect of two other inhibitors of NCX: SN-6 and Benzamil. SN-6, a benzyloxyphenyl analog, is developed from KB-R7943 and known to inhibit NCXs' reverse mode more effectively than the forward mode. SN-6 is a more selective inhibitor of NCX than KB-R7943 and at optimal concentration of 5 μ M does not affect other receptors, transporters or ion channels (38, 39). Moreover, SN-6 inhibits NCX1 more potently than NCX2 and NCX3 (38). Benzamil is an amiloride analog, which inhibits both forward and reverse mode of all three NCX isoforms (40). As shown in figure 4B, these two inhibitors reduced MUC5AC secretion compared to cells treated with vehicle alone. Importantly, the effect of SN-6 (93% reduction) was very similar to the effect of KB-R7943 (95% reduction) and much stronger than Benzamil (65% reduction), which is in accordance with our hypothesis that NCX's reverse mode, and not the other membrane currents, regulates MUC5AC secretion (Figure 4B). To further ascertain the specificity of these inhibitors, we tested the effect of SN-6 in cells depleted of NCX2. Our data show that SN-6 blocks MUC5AC secretion in control cells, but it doesn't have any additional effect on MUC5AC secretion in NCX2 KD cells (Figure S2A).

Extracellular Ca²⁺ and TRPM4 are required for MUC5AC secretion in CF cells

Our results indicate that NCX family of exchangers is required for MUC5AC secretion from colonic (HT29-18N2), bronchial (NHBE) and CF derived (CFT1-LC3) cells. Knockdown of TRPM4 affected MUC5AC secretion from HT29-18N2 cells and we asked whether it also had a role in MUC5AC secretion by CFT1-LC3 cells. To test this, we used 9-phenanthrol, which is known to

specifically inhibit TRPM4 (41). We tested its specificity in TRPM4 KD HT29-18N2 cells, and our data reveal that 9-phenanthrol inhibited MUC5AC secretion in control cells only. The effect of 9-phenanthrol treatment was not enhanced in cells depleted of TRPM4 (Figure S2B). Briefly, CFT1-LC3 differentiated cells were stimulated with a mix containing 100 μ M ATP, 10 ng/mL IL-13 and 300 nM PMA (1 hr at 37°C), resulting in a significant increase in extracellular MUC5AC (2-fold increase) that was completely abolished by 10 μ M 9-phenanthrol treatment (Figure 4C). To test the requirement of extracellular calcium in MUC5AC secretion by differentiated CFT1-LC3 cells, the cells were treated with stimuli (100 μ M ATP, 10 ng/mL IL-13 and 300 nM PMA) in the presence (1.2 mM CaCl₂) or absence (0.5 mM EGTA) of extracellular Ca²⁺ (1 hr at 37°C). As shown in figure 4D, removal of extracellular Ca²⁺ strongly reduced stimulated mucin secretion (Figure 4D). In sum, our results show that NCX's reverse mode, TRPM4 and extracellular calcium are required for MUC5AC secretion in CFT1-LC3 cells.

Discussion

Secreted mucins are the main components of mucus that protects the epithelium from pathogens, allergens and toxic compounds. The overall mechanism of how these heavily glycosylated mucins are released from the specialized epithelial goblet cells is not well understood (42). The 21 different mucins expressed in humans (endorsed by the HUGO gene nomenclature committee) can be classified into two kinds: the plasma membrane bound (transmembrane) and the gel-forming (secreted) mucins (43). The membrane-tethered mucins (like MUC1, MUC4 or MUC16) are involved in hydration and lubrication of epithelia, and protection against pathogens, whereas the secreted mucins (such as MUC5AC, MUC2 or MUC5B) are important for the formation, function and rheological properties of the mucus layer (2, 43). A screen for proteins involved in the release of MUC5AC, a secreted gel-forming mucin, by colonic goblet cancer cells revealed new candidates of which

TRPM5, a sodium channel, was described previously (11).

Our new findings reveal that the sodium importer TRPM4 and possibly its ortholog TRPM5 function via a sodium/calcium exchanger (NCX) to control mucin secretion in cells of the airways and the colon. This scheme reveals a program that regulates ATP-dependent mucin secretion by controlling calcium entry through TRPM4/TRPM5 and NCXs. It is important to note that both TRPM4 and TRPM5 sodium channels, and only NCX2, are expressed in colon cells; whereas the airway cells express TRPM4 and all 3 sodium-calcium exchangers. What is the significance of these differential combinations of TRPMs and NCXs in these tissues? We entertain the possibility that the combination of TRPM4+TRPM5 and NCX is adapted based on the stimuli to control the quantity of mucin secretion from the respective cells. In a tissue with a need for sustained mucin release to generate a large mucus layer (i.e. two mucus layers in the colon (3)), it is sufficient to utilize only one NCX, but two different sodium channels that can be activated after stimuli (to maintain the signal). In the airways, on the other hand, where a sudden increase in mucin secretion is needed to protect the tissue (i.e. after exposure to allergens or pathogens), it is important to exploit all NCX members to provoke a strong increase in calcium uptake to trigger rapid mucin secretion. Another possibility we entertain, based on our data, is that TRPM4 is the main regulator for both MUC2 and MUC5AC release from the colonic and airway cells, whereas TRPM5 likely acts as a modulator of mucin secretion and has an important role in mucous-related pathologies. Importantly, our data reveal that knockdown of TRPM4+TRPM5 and NCX has a greater effect on the physiologically secreted MUC2 by colonic cells (HT29-18N2) and MUC5AC release from the airway cells (NHBE and CFT1-LC3), respectively. MUC2 and MUC5AC are the physiologically relevant secreted mucins of the colon and airway goblet cells, respectively, so knocking down the specific isoform of TRPM and NCX expressed in these cells has a greater impact

on the secretion of corresponding mucins. MUC5AC is expressed and secreted by colonic cancer cells and not the normal colon cells, which might explain a partial effect on its secretion by TRPM4/TRPM5 and NCX knockdown. Meaning, there is an optimal pairing of the calcium import machinery and the mucins for efficient mucin secretion in a cell type specific manner.

The isoforms of these two classes of proteins involved vary in a tissue specific manner, however, the general principle is the same as described below (Figure 5). We present two albeit speculative distinct modes of mucin secretion: Baseline mucin secretion (Figure 5A) and Stimulated mucin secretion (Figure 5B).

- Baseline mucin secretion: In the absence of an external stimulus, TRPM4/TRPM5 are not active. Under these conditions, the cells control mucin secretion by coupling the function of intracellular calcium oscillations to KChIP3 (7). An increase in intracellular calcium threshold by ryanodine receptor-mediated release of calcium from the ER, loads calcium onto KChIP3 causing its release from the mature granule, which subsequently fuse to plasma membrane. This procedure is independent of low affinity calcium sensor synaptotagmin 2 (17) and used by cells to control mucin secretion in the absence of extracellular calcium (Figure 5A).

- Stimulated mucin secretion: When cells are stimulated (for example by ATP or IL-13), there is a rapid burst of Ca^{2+} released from the endoplasmic reticulum (ER), which activates TRPM4/TRPM5. Once activated, TRPM4/TRPM5 permeate sodium into the cytoplasm. The local increase in Na^+ concentration in the proximity of NCX exchangers triggers them to act in the reverse mode and pump calcium into the cells. This increases local Ca^{2+} concentration and engages the low affinity calcium sensor synaptotagmin 2 to promote fusion of mucin granules to plasma membrane (17). This procedure accounts for a rapid burst in mucin secretion under conditions such as exposure of cells to exogenous stimuli (Figure 5B).

In conclusion, our data are beginning to reveal the mechanism by which cells use intracellular vs extracellular calcium to control baseline and stimulated mucin secretion. We suggest that KChIP3 that functions in baseline secretion (7), and TRPM4/TRPM5/NCXs in stimulated mucin secretion are potential pharmacological targets to help control dysregulated mucin secretion observed in patients with diseases of the airways and the colon.

Experimental procedures

Reagents and antibodies

All chemicals were obtained from Sigma-Aldrich (St. Louis, MO) except IL-13 (R&D Systems, Minneapolis, MN), anti-MUC2 antibody clone 996/1 (RRID:AB_297837) (Abcam, Cambridge, UK) and anti-MUC5AC antibody clone 45M1 (RRID: AB_934745) (Neomarkers, Waltham, MA). Secondary antibodies for immunofluorescence microscopy and dot blotting were from Life Technologies (ThermoFisher Scientific, Waltham, MA, USA).

Cell lines

HT29-18N2 cells (from ATCC, RRID: CVCL_5942), CFT1-LC3 cells (a kind gift of Dr. J. Yankaskas, University of North Carolina at Chapel Hill) (RRID:CVCL_G214) and NHBE cells were purchased from Lonza, (Basel, Switzerland) (RRID:CVCL_S124). All cell lines were authenticated by the suppliers, and their phenotype previously demonstrated (44, 45). HT29-18N2, NHBE and CFT1-LC3 cell lines tested negative for mycoplasma contamination by the Lookout® mycoplasma PCR detection kit (Sigma-Aldrich, St. Louis, MO).

Differentiation of HT29-18N2 cells

HT29-18N2 cells were differentiated to goblet cells as described previously (11). Briefly, cells were seeded in complete growth medium (DMEM complemented with 10% FCS and 1% P/S), and the following day (D0) medium was changed to PFHMII protein free medium (GIBCO, ThermoFisher Scientific, Waltham, MA, USA). After 3 days (D3), medium was replaced with fresh PFHMII medium and cells

were grown for 3 additional days. At day 6 (D6) cells were seeded in complete growth medium for different experiments following replacement of complete growth medium for PFHMII medium at day 7 (D7). All experimental procedures were performed at day 9 (D9).

Differentiation of CF and NHBE cells

CFT1-LC3 or NHBE cells were plated in 24 mm Transwells plates with 0.4 μ m pore polyester membrane insert (Costar, Corning No. 3470, SIGMA-ALDRICH, St Louis, MO) pre-coated with Collagen type I (0.03 mg/ml) (BD Biosciences, San Jose, CA, USA). B-ALI growth medium supplemented with SingleQuots™ (according to manufacturer's instructions) (LONZA, Basel, Switzerland) was then added to both basal and apical compartment. After 3 days, medium from apical compartment was removed and medium from basal compartment was changed to B-ALI Differentiation Medium (supplemented with SingleQuots™ according to manufacturer's instructions) (LONZA, Basel, Switzerland) + IL-13 (10 ng/ml). After this time (D0) until the day of experiment (D21), the medium was changed every 3 days (See Figure 3A). From day 19 (D19) to day 21 (D21), IL-13 was removed from medium to allow goblet cells to accumulate mucin granules.

Mucin secretion assay for HT29-18N2 cells

HT29-18N2 cells were differentiated for 6 days and then split into 6-well plates. One day later (D7), the medium was exchanged with fresh PFHMII medium and cells grown for 2 more days. On D9, cells were washed with isotonic solution containing: 140 mM NaCl, 2.5 mM KCl, 1.2 mM CaCl₂, 0.5 mM MgCl₂, 5 mM glucose, and 10 mM HEPES (305 mosmol/l, pH 7.4 adjusted with Tris). The cells were then treated with 100 μ M ATP for 30 min at 37°C. Ca²⁺-free solutions were obtained by replacing CaCl₂ with equal amounts of MgCl₂ plus 0.5 mM EGTA. Supernatant was collected and centrifuged for 5 min at 800xg at 4°C. Cells were washed 2X in PBS and lysed in 2% Triton X-100 /1 mM

DTT/ PBS for 1hr at 4°C and centrifuged at 10000xg for 15 min.

Mucin secretion assay for CFT1-LC3 and NHBE cells

Mucin secretion assays for CFT1-LC3 and NHBE cells were performed on day 21 (D21), 3 days after removing IL-13 from the medium to allow the accumulation of mucins. Both apical and basolateral compartments of Transwells were washed with isotonic solution containing: 140 mM NaCl, 2.5 mM KCl, 1.2 mM CaCl₂, 0.5 mM MgCl₂, 5 mM glucose, and 10 mM HEPES (305 mosmol/l, pH 7.4 adjusted with Tris). A mix containing 100 μM ATP, 10 ng/mL IL-13 and 300 nM PMA or vehicle was then added to both compartments, and cells were incubated for 1 hr at 37°C. Medium from apical compartment was collected and centrifuged for 5 min at 800xg at 4°C (supernatant). The cells were then washed 2X in PBS (apical and basolateral sides) and lysed in 1% Triton X-100/ 1 mM DTT/ PBS for 1 hr at 4°C and centrifuged at 10000xg for 30 min (cell lysate).

Dot blot analysis

Supernatants and cell lysates were spotted on nitrocellulose membranes (0.45 μm) using Bio-Dot Microfiltration Apparatus (Bio-Rad, California, USA) (manufacturer's protocol) and membranes incubated in blocking solution (4% BSA / 0.1% Tween/ PBS) for 1 hr at room temperature. The blocking solution was removed and the membranes incubated with anti-MUC5AC antibody diluted 1:1000 or anti-MUC2 antibody diluted 1:1000 in blocking solution, overnight at 4°C. Membranes were then washed in 0.1% Tween/PBS and incubated with a donkey anti-mouse or anti-rabbit Alexa 647 coupled antibody (Life Technologies) for 30 min at room temperature. For the detection of β-actin, cell lysates were separated on SDS-PAGE, transferred to nitrocellulose membranes and processed as described for the dot blot analysis using anti-β-actin antibody (RRID:AB_476692) at a dilution of 1:5000. Membranes were washed and imaged with LI-COR Odyssey® scanner (resolution = 84 μm) (LI-COR, Nebraska, USA). Quantification of

the dot blots was performed with ImageJ (FIJI, version 2.0.0-rc-43/1.51g) (46). Linearity and specificity of MUC2 antibody in our assay are provided in Figure S3. Figure S3A shows the detection of MUC2 antibody to compare basal and stimulated secretion (Figure S3A). Figure S3B shows serial dilutions of cell lysate to determine the linearity and detection limit of our assay (Figure S3B).

Immunofluorescence analysis

Differentiated HT29-18N2 (Control, TRPM4 KD, TRPM5 KD, TRPM4+TRPM5 KD or NCX2 KD) cells were grown on coverslips. To visualize intracellular MUC5AC and MUC2 granules, differentiated HT29-18N2 cells were washed two times at room temperature with PBS for 5 min. Next, cells were permeabilized by incubation in a buffer composed of 20 mM HEPES pH 7.4, 110 mM KOAc, 2 mM MgOAc and 0.5 mM EGTA (adapted from (47)) with 0.001 mM digitonin for 5 min on ice, followed by washing for 7 min on ice with the same buffer without detergent. Then, cells were fixed in 4% paraformaldehyde for 15 min, further permeabilized for 5 min with 0.001% digitonin in the same buffer without detergent and blocked with 4% BSA in 1X PBS for 15 min. The anti-MUC5AC antibody was added to cells at 1:5000 in 4% BSA/PBS overnight at 4°C. The anti-MUC2 antibody was added to cells at 1:500 in 4% BSA/PBS overnight at 4°C. Next day, the cells were washed with PBS and incubated for 1 hr at room temperature with a donkey anti-rabbit Alexa 555 (for MUC2), anti-mouse Alexa 647 (for MUC5AC) (Life Technologies), diluted at 1:1000 in 4% BSA/PBS, and DAPI (1:20000). Finally, cells were washed in PBS and mounted in FluorSave Reagent (Calbiochem, Billerica, MA). Images were acquired using an inverted Leica SP5 confocal microscope with a 63x Plan Apo NA 1.4 objective and analyzed using ImageJ ((FIJI, version 2.0.0-rc-43/1.51g) (46). For detection, the following laser lines were applied: DAPI, 405 nm; and Alexa Fluor 555, 561 nm; Alexa Fluor 647, 647 nm.

Expression profile and qPCR

Undifferentiated and differentiated cells (HT29-18N2, NHBE and CFT1-LC3) were lysed and total RNA extracted with the RNeasy extraction kit (Qiagen, Netherlands). Total RNA was treated with Dnase I (New England Labs, Ipswich, MA) for 1 hr at 37°C and purified by phenol extraction. cDNA was synthesized with Superscript III (Invitrogen). Primers for each gene (sequence shown below, Table 1) were designed using Primer-BLAST (NCBI) (48), limiting the target size to 300 bp and the annealing temperature to 60°C. To determine expression levels of MUC5AC, NCX2, TRPM5 and TRPM4, quantitative real-time PCR was performed with Light Cycler 480 SYBR Green I Master (Roche, Switzerland) according to manufacturer's instructions.

Generation of stable shRNA knockdown cell lines

HEK293 cells (ATCC, negative for mycoplasma) were co-transfected with the plasmid, VSV-G, pPRE (packaging) and REV by calcium phosphate to produce lentiviruses. 48 hr post transfection, the secreted lentiviruses were collected, filtered and directly added to HT29-18N2 cells. Stably infected HT29-18N2 cells were selected either by puromycin resistance (10 µM) or sorted for GFP positive signal by FACS.

Measurement of intracellular [Ca²⁺]

HT29-18N2 cells were plated on glass coverslips, loaded with 5 µM of Fura-2AM for 30 min at room temperature, washed and bathed in an isotonic solution containing: 140 mM NaCl, 2.5 mM KCl, 1.2 mM CaCl₂, 0.5 mM MgCl₂, 5 mM glucose, 10 mM HEPES (305 mosmol/l, pH 7.4 adjusted with Tris). Ca²⁺-free solutions were obtained by replacing CaCl₂ with equal amounts of MgCl₂ plus 0.5 mM EGTA. Different stimuli were added to the bath solution as indicated in the figure legend. All experiments were carried out at room temperature as previously described (49). AquaCosmos software (Hamamatsu Photonics) was used for capturing the fluorescence ratio at 505 nm obtained post-excitation at 340 and 380 nm. Images were computed every 5 s. Area Under the Curve (AUC) was calculated using SigmaPlot 10 software.

Statistical analysis

All data shown are mean ± standard error of the mean (SEM). Statistical analysis was performed using Student's *t*-test (continuous data, two groups) or one-way ANOVA for the comparison of more than 2 groups (GraphPad Prism 6 (RRID:SCR_002798) or SigmaPlot 10 (RRID:SCR_003210) software). Bonferroni's test was used for post-hoc comparison of the mean values. Criteria for a significant statistical difference were: *p<0.05; **p<0.01.

Acknowledgements: We thank all members of the Malhotra Lab for valuable discussions, and Dr. J Yankaskas (University of North Carolina, Chapel Hill) for the gift of CFT1-LC3 cells. Cell sorting experiments were carried out by the joint CRG/UPF FACS Unit at Parc de Recerca Biomèdica de Barcelona (PRBB). We thank members of the Advanced Light Microscopy Unit at the CRG, Barcelona for their advice and assistance with fluorescence microscopy.

Conflict of interest: The authors declare that no competing interests exist.

Author contributions: GCR and VM conceived and designed the work; CB, NB and GCR performed the experiments; GCR analyzed the data; GCR, MAV and VM interpreted the results of the work; GCR and VM wrote the manuscript; GCR and VM were assisted by CB, NB, SM and MAV in editing and revision of the manuscript. All authors have approved the final version of the manuscript and agree to be accountable for all aspects of the work. All persons designated as authors qualify for authorship, and all those who qualify for authorship are listed.

References

1. Linden, S. K., Sutton, P., Karlsson, N. G., Korolik, V., and McGuckin, M. A. (2008) Mucins in the mucosal barrier to infection. *Mucosal Immunol.* **1**, 183–197
2. Thornton, D. J., Rousseau, K., and McGuckin, M. A. (2008) Structure and function of the polymeric mucins in airways mucus. *Annu. Rev. Physiol.* **70**, 459–486
3. Johansson, M. E. V., Larsson, J. M. H., and Hansson, G. C. (2011) The two mucus layers of colon are organized by the MUC2 mucin, whereas the outer layer is a legislator of host-microbial interactions. *Proc. Natl. Acad. Sci. U.S.A.* **108 Suppl 1**, 4659–4665
4. Rose, M. C., and Voynow, J. A. (2006) Respiratory tract mucin genes and mucin glycoproteins in health and disease. *Physiol. Rev.* **86**, 245–278
5. Adler, K. B., Tuvim, M. J., and Dickey, B. F. (2013) Regulated Mucin Secretion from Airway Epithelial Cells. *Front Endocrinol (Lausanne)*. 10.3389/fendo.2013.00129
6. Holmén Larsson, J. M., Thomsson, K. A., Rodríguez-Piñeiro, A. M., Karlsson, H., and Hansson, G. C. (2013) Studies of mucus in mouse stomach, small intestine, and colon. III. Gastrointestinal Muc5ac and Muc2 mucin O-glycan patterns reveal a regiospecific distribution. *Am. J. Physiol. Gastrointest. Liver Physiol.* **305**, G357-363
7. Cantero-Recasens, G., Butnaru, C. M., Valverde, M. A., Naranjo, J. R., Brouwers, N., and Malhotra, V. (2018) KChIP3 coupled to Ca²⁺ oscillations exerts a tonic brake on baseline mucin release in the colon. *Elife*. 10.7554/eLife.39729
8. Park, J.-A., Crews, A. L., Lampe, W. R., Fang, S., Park, J., and Adler, K. B. (2007) Protein Kinase C δ Regulates Airway Mucin Secretion via Phosphorylation of MARCKS Protein. *Am J Pathol.* **171**, 1822–1830
9. Jones, L. C., Moussa, L., Fulcher, M. L., Zhu, Y., Hudson, E. J., O’Neal, W. K., Randell, S. H., Lazarowski, E. R., Boucher, R. C., and Kreda, S. M. (2012) VAMP8 is a vesicle SNARE that regulates mucin secretion in airway goblet cells. *J. Physiol. (Lond.)*. **590**, 545–562
10. Ren, B., Azzegagh, Z., Jaramillo, A. M., Zhu, Y., Pardo-Saganta, A., Bagirzadeh, R., Flores, J. R., Han, W., Tang, Y.-J., Tu, J., Alanis, D. M., Evans, C. M., Guindani, M., Roche, P. A., Rajagopal, J., Chen, J., Davis, C. W., Tuvim, M. J., and Dickey, B. F. (2015) SNAP23 is selectively expressed in airway secretory cells and mediates baseline and stimulated mucin secretion. *Biosci. Rep.* 10.1042/BSR20150004
11. Mitrovic, S., Nogueira, C., Cantero-Recasens, G., Kiefer, K., Fernández-Fernández, J. M., Popoff, J.-F., Casano, L., Bard, F. A., Gomez, R., Valverde, M. A., and Malhotra, V. (2013) TRPM5-mediated calcium uptake regulates mucin secretion from human colon goblet cells. *Elife*. **2**, e00658
12. Guinamard, R., Sallé, L., and Simard, C. (2011) The non-selective monovalent cationic channels TRPM4 and TRPM5. *Adv. Exp. Med. Biol.* **704**, 147–171
13. Talavera, K., Yasumatsu, K., Voets, T., Droogmans, G., Shigemura, N., Ninomiya, Y., Margolskee, R. F., and Nilius, B. (2005) Heat activation of TRPM5 underlies thermal sensitivity of sweet taste. *Nature*. **438**, 1022–1025
14. Khananshvil, D. (2013) The SLC8 gene family of sodium-calcium exchangers (NCX) - structure, function, and regulation in health and disease. *Mol. Aspects Med.* **34**, 220–235
15. Rossi, A. H., Sears, P. R., and Davis, C. W. (2004) Ca²⁺ dependency of “Ca²⁺-independent” exocytosis in SPOC1 airway goblet cells. *J. Physiol. (Lond.)*. **559**, 555–565
16. Davis, C. W., and Dickey, B. F. (2008) Regulated airway goblet cell mucin secretion. *Annu. Rev. Physiol.* **70**, 487–512
17. Tuvim, M. J., Mospan, A. R., Burns, K. A., Chua, M., Mohler, P. J., Melicoff, E., Adachi, R., Ammar-Aouchiche, Z., Davis, C. W., and Dickey, B. F. (2009) Synaptotagmin 2 couples mucin granule exocytosis to Ca²⁺ signaling from endoplasmic reticulum. *J. Biol. Chem.* **284**, 9781–9787

18. Lee, H., Kim, E. K., Kim, J. Y., Yang, Y.-M., Shin, D. M., Kang, K. K., and Kim, T. (2014) DA-6034-induced mucin secretion via Ca²⁺-dependent pathways through P2Y receptor stimulation. *Invest. Ophthalmol. Vis. Sci.* **55**, 6565–6574
19. Li, D., Carozza, R. B., Shatos, M. A., Hodges, R. R., and Dartt, D. A. (2012) Effect of histamine on Ca(2+)-dependent signaling pathways in rat conjunctival goblet cells. *Invest. Ophthalmol. Vis. Sci.* **53**, 6928–6938
20. Lu, S., Liu, H., and Farley, J. M. (2011) Macrolide antibiotics inhibit mucus secretion and calcium entry in Swine airway submucosal mucous gland cells. *J. Pharmacol. Exp. Ther.* **336**, 178–187
21. Betz, A., Ashery, U., Rickmann, M., Augustin, I., Neher, E., Südhof, T. C., Rettig, J., and Brose, N. (1998) Munc13-1 is a presynaptic phorbol ester receptor that enhances neurotransmitter release. *Neuron.* **21**, 123–136
22. Abdullah, L. H., Conway, J. D., Cohn, J. A., and Davis, C. W. (1997) Protein kinase C and Ca²⁺ activation of mucin secretion in airway goblet cells. *Am. J. Physiol.* **273**, L201-210
23. Conway, J. D., Bartolotta, T., Abdullah, L. H., and Davis, C. W. (2003) Regulation of mucin secretion from human bronchial epithelial cells grown in murine hosted xenografts. *Am. J. Physiol. Lung Cell Mol. Physiol.* **284**, L945-954
24. Van Kolen, K., and Slegers, H. (2006) Integration of P2Y receptor-activated signal transduction pathways in G protein-dependent signalling networks. *Purinergic Signal.* **2**, 451–469
25. Lytton, J., Westlin, M., and Hanley, M. R. (1991) Thapsigargin inhibits the sarcoplasmic or endoplasmic reticulum Ca-ATPase family of calcium pumps. *J. Biol. Chem.* **266**, 17067–17071
26. Harper, A. G. S., and Sage, S. O. (2016) TRP-Na(+)/Ca(2+) Exchanger Coupling. *Adv. Exp. Med. Biol.* **898**, 67–85
27. Olsen, J. C., Johnson, L. G., Stutts, M. J., Sarkadi, B., Yankaskas, J. R., Swanstrom, R., and Boucher, R. C. (1992) Correction of the apical membrane chloride permeability defect in polarized cystic fibrosis airway epithelia following retroviral-mediated gene transfer. *Hum. Gene Ther.* **3**, 253–266
28. Vázquez, E., Nobles, M., and Valverde, M. A. (2001) Defective regulatory volume decrease in human cystic fibrosis tracheal cells because of altered regulation of intermediate conductance Ca²⁺-dependent potassium channels. *Proc. Natl. Acad. Sci. U.S.A.* **98**, 5329–5334
29. Kreda, S. M., Davis, C. W., and Rose, M. C. (2012) CFTR, mucins, and mucus obstruction in cystic fibrosis. *Cold Spring Harb Perspect Med.* **2**, a009589
30. Gray, T. E., Guzman, K., Davis, C. W., Abdullah, L. H., and Nettekheim, P. (1996) Mucociliary differentiation of serially passaged normal human tracheobronchial epithelial cells. *Am. J. Respir. Cell Mol. Biol.* **14**, 104–112
31. Dickinson, J. D., Alevy, Y., Malvin, N. P., Patel, K. K., Gunsten, S. P., Holtzman, M. J., Stappenbeck, T. S., and Brody, S. L. (2016) IL13 activates autophagy to regulate secretion in airway epithelial cells. *Autophagy.* **12**, 397–409
32. Kimura, J., Watano, T., Kawahara, M., Sakai, E., and Yatabe, J. (1999) Direction-independent block of bi-directional Na⁺/Ca²⁺ exchange current by KB-R7943 in guinea-pig cardiac myocytes. *Br. J. Pharmacol.* **128**, 969–974
33. Iwamoto, T., Kita, S., Uehara, A., Inoue, Y., Taniguchi, Y., Imanaga, I., and Shigekawa, M. (2001) Structural domains influencing sensitivity to isothiourea derivative inhibitor KB-R7943 in cardiac Nna(+)/Ca(2+) exchanger. *Mol. Pharmacol.* **59**, 524–531
34. Arakawa, N., Sakaue, M., Yokoyama, I., Hashimoto, H., Koyama, Y., Baba, A., and Matsuda, T. (2000) KB-R7943 inhibits store-operated Ca(2+) entry in cultured neurons and astrocytes. *Biochem. Biophys. Res. Commun.* **279**, 354–357

35. Sobolevsky, A. I., and Khodorov, B. I. (1999) Blockade of NMDA channels in acutely isolated rat hippocampal neurons by the Na⁺/Ca²⁺ exchange inhibitor KB-R7943. *Neuropharmacology*. **38**, 1235–1242
36. Pintado, A. J., Herrero, C. J., García, A. G., and Montiel, C. (2000) The novel Na⁽⁺⁾/Ca⁽²⁺⁾ exchange inhibitor KB-R7943 also blocks native and expressed neuronal nicotinic receptors. *Br. J. Pharmacol.* **130**, 1893–1902
37. Matsuda, T., Arakawa, N., Takuma, K., Kishida, Y., Kawasaki, Y., Sakaue, M., Takahashi, K., Takahashi, T., Suzuki, T., Ota, T., Hamano-Takahashi, A., Onishi, M., Tanaka, Y., Kameo, K., and Baba, A. (2001) SEA0400, a novel and selective inhibitor of the Na⁺-Ca²⁺ exchanger, attenuates reperfusion injury in the in vitro and in vivo cerebral ischemic models. *J. Pharmacol. Exp. Ther.* **298**, 249–256
38. Iwamoto, T., Inoue, Y., Ito, K., Sakaue, T., Kita, S., and Katsuragi, T. (2004) The exchanger inhibitory peptide region-dependent inhibition of Na⁺/Ca²⁺ exchange by SN-6 [2-[4-(4-nitrobenzyloxy)benzyl]thiazolidine-4-carboxylic acid ethyl ester], a novel benzyloxyphenyl derivative. *Mol. Pharmacol.* **66**, 45–55
39. Niu, C.-F., Watanabe, Y., Ono, K., Iwamoto, T., Yamashita, K., Satoh, H., Urushida, T., Hayashi, H., and Kimura, J. (2007) Characterization of SN-6, a novel Na⁺/Ca²⁺ exchange inhibitor in guinea pig cardiac ventricular myocytes. *Eur. J. Pharmacol.* **573**, 161–169
40. Watanabe, Y., Koide, Y., and Kimura, J. (2006) Topics on the Na⁺/Ca²⁺ exchanger: pharmacological characterization of Na⁺/Ca²⁺ exchanger inhibitors. *J. Pharmacol. Sci.* **102**, 7–16
41. Guinamard, R., Hof, T., and Del Negro, C. A. (2014) The TRPM4 channel inhibitor 9-phenanthrol. *Br. J. Pharmacol.* **171**, 1600–1613
42. Birchenough, G. M. H., Johansson, M. E. V., Gustafsson, J. K., Bergström, J. H., and Hansson, G. C. (2015) New developments in goblet cell mucus secretion and function. *Mucosal Immunol.* **8**, 712–719
43. Hattrup, C. L., and Gendler, S. J. (2008) Structure and function of the cell surface (tethered) mucins. *Annu. Rev. Physiol.* **70**, 431–457
44. Phillips, T. E., Ramos, R., and Duncan, S. L. (1995) HT29-18N2 differentiation in a protein-free medium. *In Vitro Cell. Dev. Biol. Anim.* **31**, 421–423
45. Yankaskas, J. R., Haizlip, J. E., Conrad, M., Koval, D., Lazarowski, E., Paradiso, A. M., Rinehart, C. A., Sarkadi, B., Schlegel, R., and Boucher, R. C. (1993) Papilloma virus immortalized tracheal epithelial cells retain a well-differentiated phenotype. *Am. J. Physiol.* **264**, C1219-1230
46. Schindelin, J., Arganda-Carreras, I., Frise, E., Kaynig, V., Longair, M., Pietzsch, T., Preibisch, S., Rueden, C., Saalfeld, S., Schmid, B., Tinevez, J.-Y., White, D. J., Hartenstein, V., Eliceiri, K., Tomancak, P., and Cardona, A. (2012) Fiji: an open-source platform for biological-image analysis. *Nat. Methods*. **9**, 676–682
47. Lorenz, H., Hailey, D. W., and Lippincott-Schwartz, J. (2008) Addressing membrane protein topology using the fluorescence protease protection (FPP) assay. *Methods Mol. Biol.* **440**, 227–233
48. Ye, J., Coulouris, G., Zaretskaya, I., Cutcutache, I., Rozen, S., and Madden, T. L. (2012) Primer-BLAST: a tool to design target-specific primers for polymerase chain reaction. *BMC Bioinformatics*. **13**, 134
49. Fernandes, J., Lorenzo, I. M., Andrade, Y. N., Garcia-Elias, A., Serra, S. A., Fernández-Fernández, J. M., and Valverde, M. A. (2008) IP₃ sensitizes TRPV4 channel to the mechano- and osmotransducing messenger 5'-6'-epoxyeicosatrienoic acid. *J. Cell Biol.* **181**, 143–155

FOOTNOTES

Funding: We acknowledge support of the Spanish Ministry of Economy and Competitiveness, through the Programmes ‘Centro de Excelencia Severo Ochoa 2013-2017’ (SEV-2012-0208) and Maria de Maeztu Units of Excellence in R&D (MDM-2015-0502); and under grant agreement FPDI-2013-16916 to G Cantero-Recasens. The research leading to these results has received funding from Spanish Ministry of Economy and Competitiveness under grant agreement SAF2015-69762R to MA Valverde. This work reflects only the authors’ views and the Community is not liable for any use that may be made of the information contained therein. Vivek Malhotra is an Institució Catalana de Recerca i Estudis Avançats (ICREA) professor at the Center for Genomic Regulation in Barcelona, and the work in his laboratory is funded by grants from MINECO’s Plan Nacional (BFU2013-44188-P) and Consolider (CSD2009-00016).

The abbreviations used are: CF, cystic fibrosis; MUC5AC, mucin-5AC; MUC2, mucin-2; NCX, sodium-calcium exchanger; NHBE, normal human bronchial epithelial cells; PMA, phorbol-12-myristate-13-acetate; TRPM4, transient receptor potential cation channel subfamily M member 4; TRPM5, transient receptor potential cation channel subfamily M member 5

TABLES

Table 1. Primer sequences used for detecting mRNA for the respective genes

Gene	Forward primer (5' - 3')	Reverse primer (3' - 5')
SLC8A1	CTTGTGGAGAGCTCGAATTCAG	CTCTTCCTCTTTGCTGGTCAGTGG
SLC8A2	GGGATTTTCAGCTCTGCTACTCAA	CGCTCACCGTAATTGCCTCTAAA
SLC8A3	TCATCGTCCCCTTTAGGACAGT	CCTCTTCTTCCATAGTCAGCTTCC
MUC5AC	CACTTCTCAACGTTTGACGGGA	CTTGATCACCACCACCGTCTG
MUC2	TGTAGGCATCGCTCTTCTCA	GACACCATCTACCTCACCCG
TRPM4	CAAAAGAAGGCGAGAACCA	CCTCTTTGGCGAGTGCTATC
TRPM5	CCAGAAGGAGAACTTCCTGAGC	GGTTGTTCCCAGCCATCTAAAC
HPRT1	CCTGCTTCTCCTCAGCTTCAG	ACACCCTTTCCAAATCCTCAGC
GAPDH	GAAGGTGAAGGTCGGAGTCAAC	CATCGCCCCACTTGATTTTGGGA

FIGURE LEGENDS

Figure 1. TRPM4/TRPM5 and NCX2 are required for mucin secretion by HT29-18N2 colonic cancer cells. (A) RNA levels of NCX1, NCX2, NCX3, TRPM4, TRPM5, MUC2 and MUC5AC in positive control cDNA (control cDNA for NCX1, NCX2, TRPM4; lungs cDNA for NCX3, TRPM5 and MUC5AC; and colon cDNA for MUC2; MTC cDNA Panels, Clontech Laboratories) and differentiated HT29-18N2 cDNA were analyzed by agarose gel. (B) Intracellular MUC5AC levels of control, TRPM4, TRPM5, TRPM4+TRPM5, and NCX2 KD cells. Differentiated cells were lysed and analyzed by dot blot with an anti-MUC5AC and anti-actin antibody. Intensities of MUC5AC spots were normalized to the actin levels. Results are means \pm SEM (N \geq 3). (C) Intracellular MUC2 levels of differentiated control, TRPM4 KD, TRPM5 KD, TRPM4+TRPM5 KD and NCX2 KD cells. Cells were lysed and analyzed by dot blot with an anti-MUC2 and anti-actin antibody. Intensities of MUC2 spots were quantified using ImageJ and normalized to the actin levels. Results are means \pm SEM (N = 3). (D) Control, TRPM4, TRPM5, TRPM4+TRPM5 and NCX2 stable knockdown cells were starved and incubated for 30 min at 37°C with 100 μ M ATP or vehicle. Secreted MUC5AC was collected, processed for dot blot analysis with an anti-

MUC5AC antibody and quantified using ImageJ. The y-axis represents relative values with respect to the values of untreated cells of each condition. Average values \pm SEM are plotted as bar graphs ($N \geq 3$). Statistics are showed for 100 μ M ATP condition. (E) Differentiated control, TRPM4 KD, TRPM5 KD, TRPM4+TRPM5 KD and NCX2 KD cells were incubated for 30 min at 37°C with 100 μ M ATP or vehicle. Secreted MUC2 was collected and analyzed by dot blot with an anti-MUC2 antibody and analyzed with ImageJ. The y-axis of the plot represents relative values with respect to the values of untreated cells for each condition. Average values \pm SEM are plotted as bar graphs ($N = 3$). Statistical analyses are only shown for 100 μ M ATP stimulation. (F) Control, TRPM4 KD, TRPM5 KD, TRPM4+TRPM5 KD and NCX2 KD cells were differentiated by starvation. After starvation, cells were processed for cytosolic washout, fixed and permeabilized for analysis by immunofluorescence microscopy with an anti-MUC5AC antibody (red), anti-MUC2 antibody (green) and DAPI (blue). Scale bar = 5 μ m. Abbreviations: Ctrl: Control, Neg: reverse transcription without reverse transcriptase, Scr.: Scrambled shRNA, TRPM4/5 shRNA: TRPM4+TRPM5 KD cells. * $p < 0.05$, ** $p < 0.01$.

Figure 2. TRPM4/5 and NCX control ATP-mediated Ca^{2+} entry. (A) HT29-18N2 cells were starved for 6 days and incubated for 30 min at 37°C with 100 μ M ATP or vehicle in the presence or absence of extracellular Ca^{2+} . Secreted MUC5AC was collected and processed for dot blot analysis with an anti-MUC5AC antibody. The dot blots were quantified using ImageJ. The y-axis represents relative values with respect to the values of vehicle treated cells for each condition. Average values \pm SEM are plotted as bar graphs ($N=3$). (B) Secreted medium from differentiated HT29-18N2 after treatment with 100 μ M ATP or the vehicle in the presence or absence of extracellular Ca^{2+} was processed for dot blot analysis with an anti-MUC2 antibody. The y-axis represents relative values with respect to the values of vehicle treated cells for each condition. Average values \pm SEM are plotted as bar graphs ($N=3$). (C) Time course of mean Ca^{2+} responses (normalized FURA-2AM ratio) obtained in differentiated HT29 cells treated with 100 μ M ATP (black dots) or 1 μ M TG (white dots) ($N > 3$) in the absence (Calcium release from internal stores) or presence (Calcium entry) of 1.2 mM $CaCl_2$. (D) Average AUC (Area Under the Curve) from the traces shown in panel C in the absence of Ca^{2+} (Stores release, AUC for 8 min) or in the presence of extracellular Ca^{2+} (Ca^{2+} entry, AUC for 10 min). (E) Differentiated HT29-18N2 cells were incubated for 30 min at 37°C with 100 μ M ATP, 1 μ M TG or vehicle. Secreted MUC5AC was collected and processed for dot blot with an anti-MUC5AC antibody. The y-axis represents relative values to vehicle condition. Results are average values \pm SEM ($N=3$). (F) Time course of mean Ca^{2+} responses (normalized FURA-2AM ratio) obtained in differentiated HT29-18N2 cells (Control, TRPM4 KD, TRPM5 KD, TRPM4+TRPM5 KD and NCX2 KD) treated with 100 μ M ATP ($N \geq 3$) in absence (stores release) or presence (Ca^{2+} entry) of extracellular Ca^{2+} . (D) Average AUC (Area Under the Curve, 5 min for Stores release, 10 min for Ca^{2+} entry) obtained from traces shown in C. Abbreviations: Veh: Vehicle, TG: Thapsigargin, TRPM4/5 shRNA: TRPM4+TRPM5 KD cells. ** $p < 0.01$.

Figure 3. Differentiation of Airway Cells. (A) Schematic representation of airlift differentiation protocol. (B) Total RNA was extracted from undifferentiated (UND) and 21-day differentiated (DIF) NHBE and CFT1-LC3 cells. RNA levels of *MUC5AC* were monitored by qPCR (*GAPDH* was used as a reference gene) (C) Undifferentiated and 21-day differentiated NHBE and CFT1-LC3 cells were lysed and the lysates analyzed by dot blot with an anti-MUC5AC antibody. The intensity of the spots was quantified using ImageJ and normalized and normalized to β -actin levels and to undifferentiated cells. Results are means \pm SEM ($N=3$). (D) Undifferentiated and 21-day differentiated NHBE and CFT1-LC3 cells were treated for 1 hr at 37°C with stimuli. Secreted MUC5AC was collected and analyzed by dot blot with an anti-MUC5AC antibody. The dot blots were quantified using ImageJ. Results are means \pm SEM ($N=3$). (E) Total RNA was

extracted from 21-day differentiated NHBE and CFT1-LC3 cells. RNA levels of NCX1, NCX2, NCX3, TRPM4, TRPM5 and MUC5AC were analyzed by agarose gel electrophoresis. *HPRT1* was used as a loading control. Abbreviations: IL-13: Interleukin 13, UND: Undifferentiated, DIF: Differentiated, D21: Day 21, Neg: Negative, Ext.: Extraction. * $p < 0.05$, ** $p < 0.01$.

Figure 4. Involvement of NCXs in MUC5AC secretion by airway cells. (A) Differentiated NHBE cells were pretreated for 15 min at 37°C with DMSO (Control) or 50 μM KB-R7943 (NCX inh.). After 15 min, a mix containing 100 μM ATP + 10 ng/mL IL-13 + 300 nM PMA, and the respective drug (DMSO or KB-R7943) was added to the cells and incubated for 1 hr at 37°C. Secreted MUC5AC was collected and processed for dot blot with an anti-MUC5AC antibody. The y-axis represents relative values with respect to the values of the basal of each condition. Results are average values \pm SEM ($N \geq 3$). (B) Differentiated CFT1-LC3 cells were pretreated for 15 min at 37°C with DMSO (Control), 50 μM KB-R7943 (KB-R), 5 μM Benzamil (Benz.) or 5 μM SN-6. After 15 min, a mix containing 100 μM ATP + 10 ng/mL IL-13 + 300 nM PMA, and the respective drug (DMSO, KB-R7943, Benzamil or SN-6) was added to the cells and incubated for 1 hr at 37°C. Secreted MUC5AC was collected and processed for dot blot with an anti-MUC5AC antibody. The y-axis represents relative values with respect to the values of the basal of each condition. Results are average values \pm SEM ($N \geq 4$). (C) Differentiated CFT1-LC3 cells were incubated for 1h at 37°C with DMSO (Control) or 10 μM 9-phenanthrol (TRPM4 inh.) in the presence or absence of stimuli (100 μM ATP + 10 ng/mL IL-13 + 300 nM PMA). Secreted MUC5AC was collected and processed for dot blot with an anti-MUC5AC antibody. The y-axis represents relative values with respect to the values of the basal for each condition. Results are average values \pm SEM ($N \geq 3$). (D) CFT1-LC3 differentiated cells were incubated for 1h at 37°C with a mix containing 100 μM ATP + 10 ng/mL IL-13 + 300 nM PMA or vehicle in the presence (w/ Ca^{2+}) or absence of Ca^{2+} (wo/ Ca^{2+}). Secreted MUC5AC was collected and processed for dot blot analysis with an anti-MUC5AC antibody. The dot blots were quantified using ImageJ. The y-axis represents relative values with respect to the values of vehicle treated cells for each condition. Average values \pm SEM are plotted as bar graphs ($N=3$). Abbreviations: NCX inh.: NCX inhibitor KB-R7943, TRPM4 inh.: TRPM4 inhibitor 9-phenanthrol, w/: with, wo/: without. * $p < 0.05$, ** $p < 0.01$

Figure 5. A working model for MUC5AC secretion. (A) Baseline mucin secretion. In the absence of an external stimulus, TRPM4/TRPM5 are inactive. The secretion of mucin under these conditions is regulated by KChIP3 and intracellular calcium oscillations (7). (B) Stimulated mucin secretion. After stimulation with an exogenous stimulus, TRPM4/TRPM5 are active and permit sodium into the cell. This pool of Na^+ triggers NCX to operate in the reverse mode whereby Na^+ is pumped out and Ca^{2+} is imported into the cytoplasm. The local increase in Ca^{2+} by this procedure triggers mucin secretion. Abbreviations: Rec: Receptor, IP₃R: Inositol 1,4,5-trisphosphate receptor, NCX: Sodium-Calcium exchanger, Ext: extracellular, Cyt: cytosol, ER: Endoplasmic Reticulum.

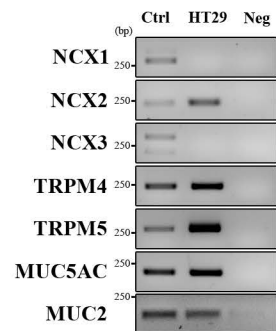
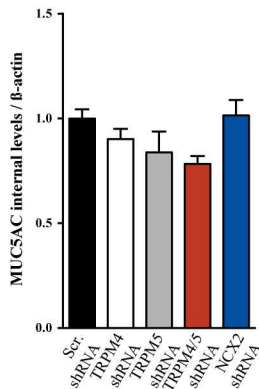
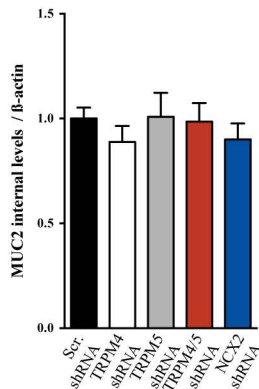
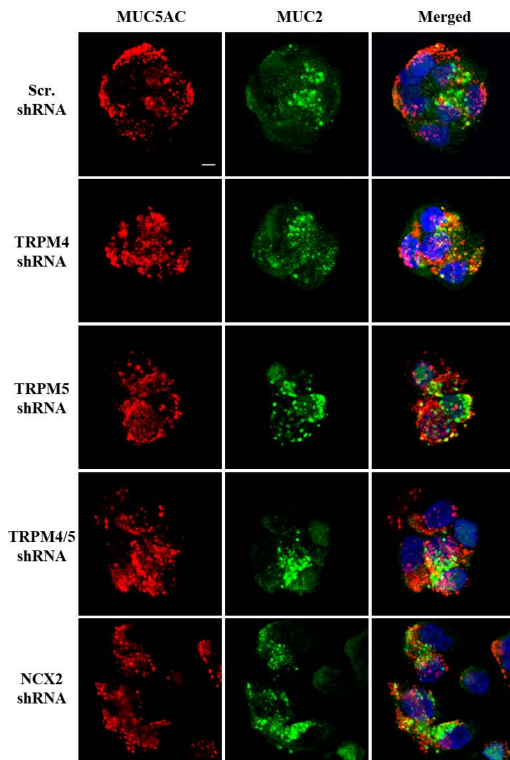
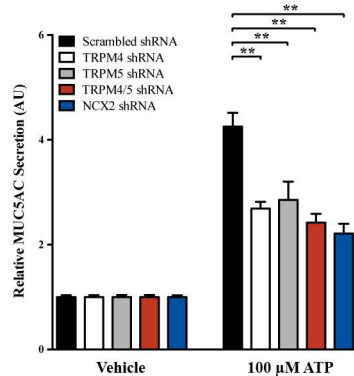
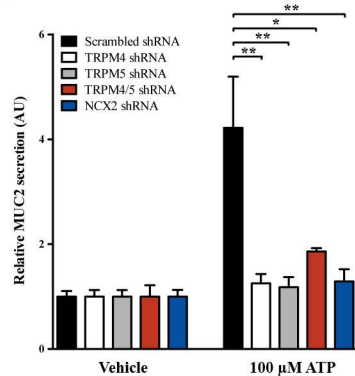
FIGURE 1**A.****B.****C.****E.****D.****E.**

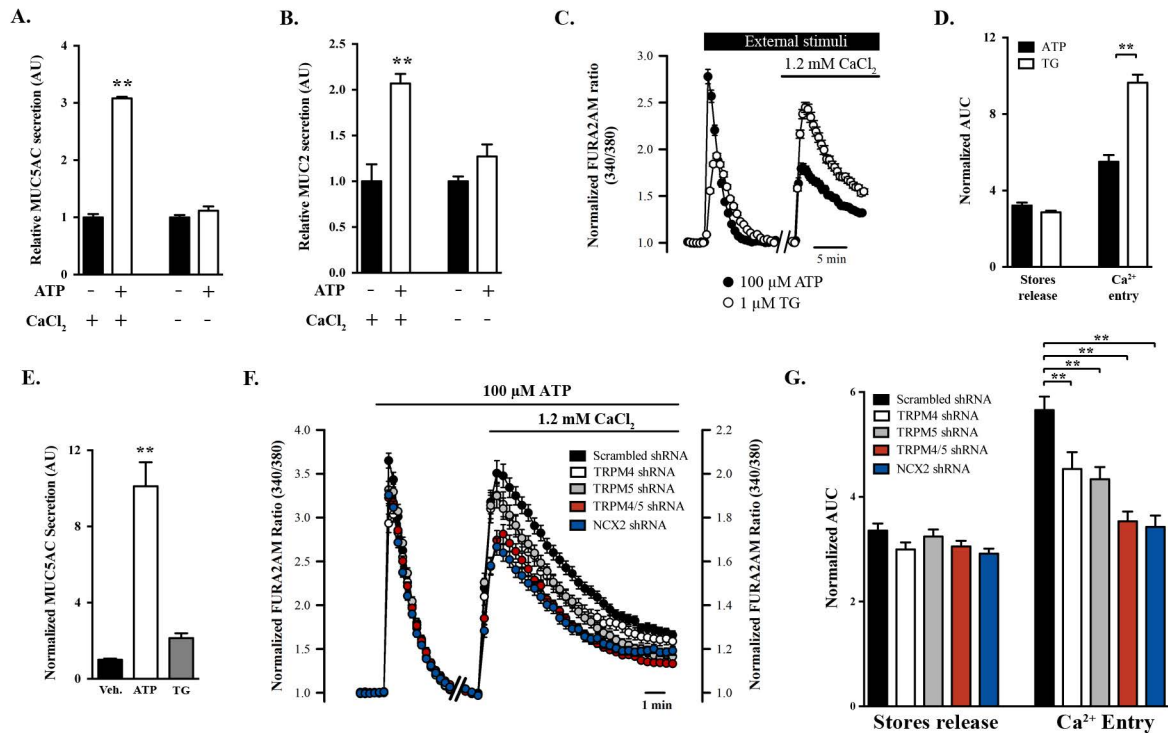
FIGURE 2

FIGURE 3

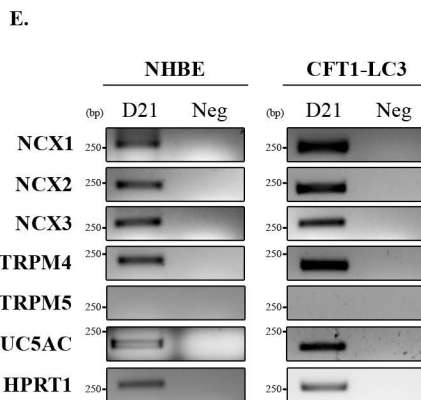
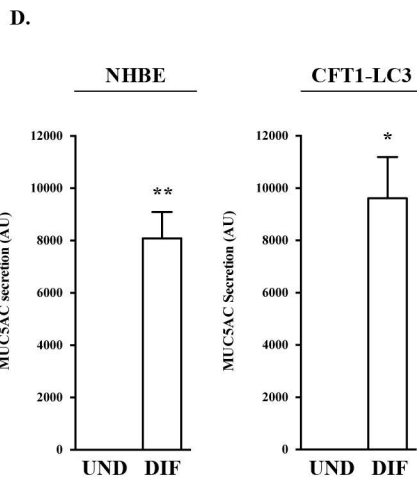
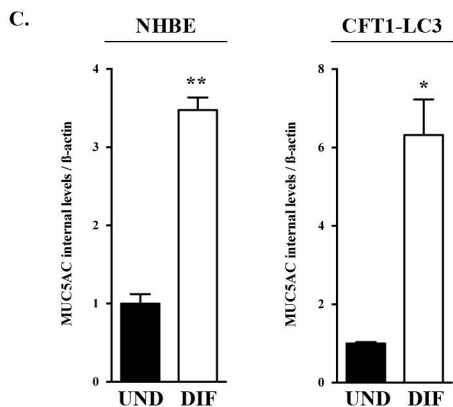
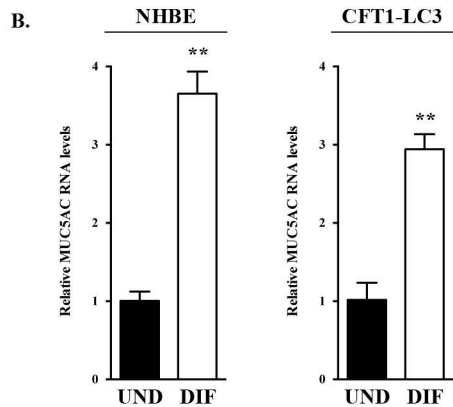
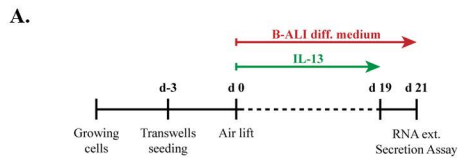


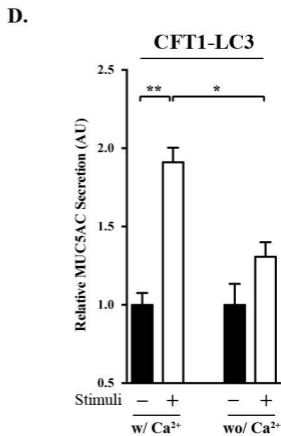
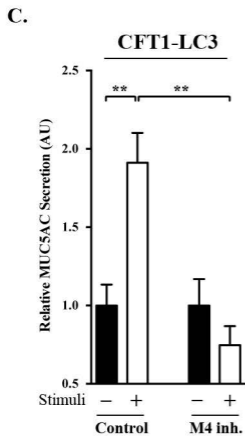
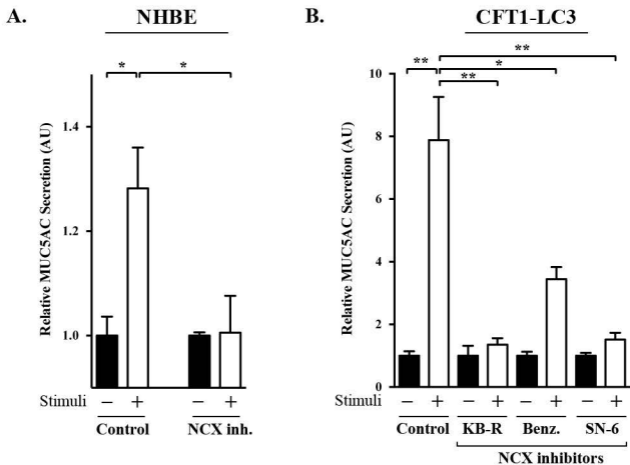
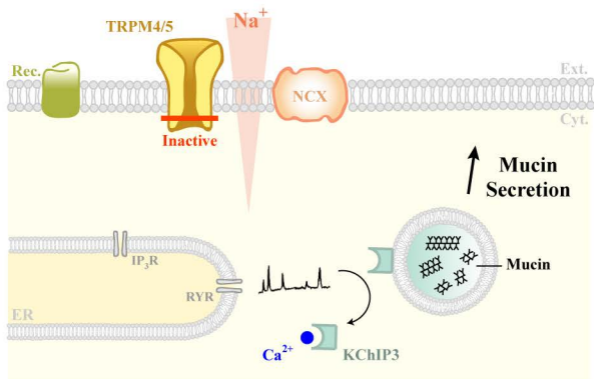
FIGURE 4

FIGURE 5

A. BASELINE MUCIN SECRETION



B. STIMULATED MUCIN SECRETION

